ORIGINAL ARTICLE

Zoologica Scripta | WILEY

The *Phyllotis xanthopygus* complex (Rodentia, Cricetidae) in central Andes, systematics and description of a new species

J. Pablo Jayat[1] | **Pablo Teta**[2] | **Agustina A. Ojeda**[3] | **Scott J. Steppan**[4] | **Jared M. Osland**[4] | **Pablo E. Ortiz**[5] | **Agustina Novillo**[6] | **Cecilia Lanzone**[7] | **Ricardo A. Ojeda**[3]

[1]Unidad Ejecutora Lillo, CONICET-Fundación M. Lillo, Tucumán, Argentina

[2]CONICET, División Mastozoología, Museo Argentino de Ciencias Naturales "Bernardino Rivadavia", Ciudad Autónoma de Buenos Aires, Argentina

[3]Grupo de Investigaciones de la Biodiversidad-IADIZA-CCTMendoza-CONICET, Mendoza, Argentina

[4]Department of Biological Science, Florida State University, Tallahassee, FL, USA

[5]Instituto Superior de Correlación Geológica, CONICET – Universidad Nacional de Tucumán, San Miguel de Tucumán, Argentina

[6]Instituto de Biodiversidad Neotropical (IBN), CCT-CONICET, Tucumán, Argentina

[7]Laboratorio de Genética Evolutiva, IBS (CONICET-UNaM), Posadas, Argentina

Correspondence
J. Pablo Jayat, Unidad Ejecutora Lillo (CONICET- Fundación Miguel Lillo). Miguel Lillo 251. CP 4000. San Miguel de Tucumán, Tucumán, Argentina.
Email: eljayat@gmail.com

Abstract

Phyllotis Waterhouse 1837 is one of the most studied genera of South American cricetid rodents. As currently understood, it includes 20 small to medium-sized species of predominantly rocky habitats. Among them, populations of the yellow-rumped leaf-eared mouse, traditionally referred to *P. xanthopygus* (Waterhouse 1837), are the most widely distributed, extending from central Peru to southern Chile and Argentina. Based mostly on molecular evidence, previous studies suggested that *P. xanthopygus* constitutes a species complex, being characterized by geographically structured and genetically divergent clades. In this work, we compare the molecular phylogenetic hypothesis for populations distributed on the eastern slopes of the central Andes with morphometric evidence using univariate and multivariate analyses. Quantitative morphological and molecular evidence suggests that at least four nearly cryptic species of the *P. xanthopygus* complex occur from southern Bolivia to west-central Argentina. Three of these taxa have available names; one of them, *P. caprinus*, is currently recognized to the species level; the other two, the clades of *P. x. posticalis-P. x. rupestris* and *P. vaccarum*, are both recognized as subspecies of *P. xanthopygus*. The remaining taxon represents a new species distributed in the west-central Andes of Argentina. We discuss our morphological results in the light of other sources of evidence (e.g. qualitative and quantitative state characters, genetic and phylogenetic studies, and cytogenetic data) and name the new species as *P. pehuenche*, honouring the original native people that historically inhabited west-central Andes of Argentina.

KEYWORDS
cryptic species, integrative taxonomy, Myomorpha, new species, Phyllotini, sigmodontinae

1 | INTRODUCTION

The leaf-eared mice of the genus *Phyllotis* Waterhouse 1837 include 20 species of small to medium-sized sigmodontine rodents found mainly in rocky habitats (Jayat et al., 2016; Rengifo & Pacheco, 2015; Steppan & Ramírez, 2015). The geographic distribution of this genus extends widely in South America, from the highlands of Ecuador, throughout the Andes and Andean foothills, to the southern tip of the continent (Steppan & Ramírez, 2015). Most species of *Phyllotis* inhabit open, arid to semiarid, mostly rocky and brushy habitats, from sea level up to over 6,700 m (Steppan & Ramírez, 2015; Storz et al., 2020), but a few species are associated with more humid and forested areas of Yungas environments, on eastern sub-Andean slopes (Ferro et al., 2010; Jayat et al., 2007; Jayat et al., 2016). Furthermore, isolated populations of these mice are distributed in montane grassland habitats of the Sierras Pampeanas and the Sierra de la Ventana, in central and east-central Argentina, respectively (Crespo, 1964; Pearson, 1972; Steppan & Ramírez, 2015; Teta et al., 2018).

Several systematic studies, based both on morphological and molecular data, have contributed to clarifying most of the phylogenetic relationships, species boundaries and taxonomy among the species of this genus (e.g. Ferro et al., 2010; Jayat et al., 2007; Jayat et al., 2016; Steppan, 1995, 1998; Steppan et al., 2007; Pacheco et al., 2014; Rengifo & Pacheco, 2015, 2017; Ojeda et al., 2021). All these studies have substantially expanded our understanding of the species-level taxonomy of the genus, but several uncertainties still remain, especially for populations representing the nominal forms described for central and southern Andean areas (Ojeda et al., 2021).

Based on morphological and molecular evidence, three species groups are currently recognized within *Phyllotis*: the *andium-amicus*, the *osilae* and the *darwini* groups (Rengifo & Pacheco, 2017; Steppan, 1993, 1995; Steppan et al., 2007). The *P. darwini* species group, which is the most speciose, includes *P. darwini* (Waterhouse 1837), *P. bonariensis* Crespo, 1964, *P. caprinus* Pearson, 1958, *P. limatus* Thomas, 1912, *P. magister* Thomas, 1912, *P. osgoodi* Mann 1945 and *P. xanthopygus* (Waterhouse 1837). Among these, the yellow-rumped leaf-eared mouse, *P. xanthopygus*, is the most widely distributed species (having the largest altitudinal range of any vertebrate), occurring from Junín department, in central Peru to the provinces of Magallanes and Santa Cruz in southern Chile and Argentina, respectively. Across this 6,000 km range, populations assigned to *P. xanthopygus* are often the most common rodent species among small mammal assemblages (Steppan & Ramírez, 2015). Although this rodent shows an apparently continuous geographic distribution across the arid and semiarid Andean ecosystems, some geographically isolated populations

occur in central Argentina, within temperate grassland environments (Ojeda et al., 2021; Steppan & Ramírez, 2015; Teta et al., 2018).

The complex taxonomic history of the nominal forms related to *P. xanthopygus* has been extensively documented in several publications (e.g. Hershkovitz, 1962; Ojeda et al., 2021; Pearson, 1958; Steppan & Ramírez, 2015; Teta et al., 2018); here, we will provide a brief resume, but readers interested in going further into this topic should consult basic literature. Pearson (1958) and Hershkovitz (1962), in his revision of the genus, considered *P. darwini* as a widely distributed and polytypic species, including the nominal forms *xanthopygus*, *chilensis* Mann 1945, *posticalis* Thomas, 1912, *ricardulus* Thomas, 1919, *rupestris* P. Gervais 1841, *limatus* Thomas, 1912 and *vaccarum* Thomas, 1912 as subspecies (later, Crespo [1964] added the nominal form *bonariensis*). Based on karyotypic and crossbreeding evidence, Walker et al. (1984) proved that true *P. darwini* is geographically restricted to central Chile, leaving all the other nominal taxa under *P. xanthopygus*. Since then, the status of *P. xanthopygus* underwent additional removal of the nominal forms *bonariensis* and *limatus*, which were both considered as valid species (e.g. Reig, 1978; Steppan, 1998; Steppan & Ramírez, 2015). Finally, an important milestone should be mentioned; recent molecular studies have challenged the traditional classification of *xanthopygus* into six subspecies, showing that, as it is currently understood, this taxon is a complex of two or more cryptic species (Albright, 2004; Jayat et al., 2016; Ojeda et al., 2021; Riverón, 2011). The taxonomy of most of the nominal forms related to the *P. xanthopygus* complex was initially addressed using morphology (e.g. Hershkovitz, 1962; Pearson, 1958). However, inconsistencies between these taxonomic delimitations and more recent molecular analyses have become evident (see Teta et al., 2018 and Ojeda et al., 2021). In this context, the integration of existing molecular results with additional sources of data (e.g. morphological, cytogenetic) seems to be the next step in delimiting species and resolving the taxonomic status of some nominal forms (e.g. *ricardulus* Thomas, 1919, *oreigenus* Cabrera, 1926 and *darwinii vaccarum* Thomas, 1912).

The aim of our study was to test the taxonomic status of the main clades obtained in the most recent molecular phylogenetic hypothesis for the *P. xanthopygus* complex (Ojeda et al., 2021) primarily using morphological evidence but supplemented with new DNA sequence data. The molecular analyses of Ojeda et al. (2021) recovered eight well supported monophyletic groups, with two major clades in the species complex. One included *P. xanthopygus s.s.*, *P. bonariensis*, *P. caprinus*, *P. limatus,* and *P. vaccarum*, and two additional clades named *P.* sp. 1, and *P.* sp. 2. The other was a diverse clade of specimens from different populations and localities

from the Altiplano of northern Argentina, northern Chile, Bolivia and southern Peru, named the *P. posticalis-P. rupestris* clade. Using a unilocus species delimitation method, the Bayesian implementation of the Poisson tree processes (bPTP), these authors corroborate most of these clades as species-level lineages, but four species were delimited within the clade of *P. posticalis – P. rupestris*. The mean genetic distances between clades ranged from 3.0% between *P. vaccarum* and *P. limatus*, to 10.6% between *P.* sp. 1 and *P.* sp. 2 and between *P. posticalis-P. rupestris* and *P.* sp. 2.

In this work, we use morphology to test the status of those clades distributed on the eastern Andean slopes of the west-central Andes of Argentina, which include, from north to south, *P. x. posticalis - P. x. rupestris*, *P. caprinus*, *P. vaccarum* and *P.* sp. 2. We focus our analysis on populations of the central Andes in western Argentina because is a geographic area highly underrepresented in previous studies and for which we have gathered a great quantity of information in recent years. We characterize at least four clades that we hypothesize correspond to distinct species. Three of these clades could be associated with previously available names but we recognize one as representing a new species. We discuss our results in the light of other sources of evidence (including genetic, phylogenetic and cytogenetic published data) and describe the newly recognized species, which was named honouring the original native people that historically inhabited west-central Andes of Argentina and nearby areas of Chile.

2 | MATERIALS AND METHODS

2.1 | Specimens examined

Specimens of *Phyllotis* used in this study (Figure 1 and Supplementary Material S1) are housed in the following Argentinean natural history collections: Centro Regional de Investigaciones Científicas y Transferencia Tecnológica de La Rioja (CRILAR), La Rioja; Instituto Argentino de Investigaciones de Zonas Áridas (CMI), Mendoza; Fundación-Instituto Miguel Lillo (CML), San Miguel de Tucumán; Museo Argentino de Ciencias Naturales 'Bernardino Rivadavia' (MACN-Ma), Ciudad Autónoma de Buenos Aires; Museo Municipal de Ciencias Naturales 'Lorenzo Scaglia' (MMPMa), Mar del Plata; Centro Nacional Patagónico (CNP), Puerto Madryn. We examined 654 specimens of this genus, including types and topotypes of several nominal forms allied to the *P. xanthopygus* species complex, including *P. bonariensis* Crespo, 1964 (holotype and paratypes); *P. caprinus* Pearson, 1958 (topotypes); *P. darwini vaccarum* Thomas, 1912 (topotypes); *P. ricardulus* Thomas, 1919 (topotypes); and *P. oreigenus* Cabrera, 1926 (topotypes).

### 2.2 | Phylogenetic framework of the study

We structured all qualitative and quantitative morphologic analyses on the basis of the phylogenetic hypothesis developed by Ojeda et al. (2021). Additionally, we added 47 new samples not included in Ojeda et al. (2021) that greatly expanded the geographic coverage for DNA data and analysed them in a more restricted and detailed genealogic analysis, testing the monophyly of the new species (see Supplementary Material S1).

2.3 | Taxonomic assignment of the samples

We examined skull and dental morphology of the Argentinean specimens of *Phyllotis* used in the phylogenetic analysis developed by Ojeda et al. (2021) in search of qualitative state characters associated to each one of the recognized mitochondrial clades. Then, we looked for these same characters in the specimens examined in systematic collections not included in the phylogenetic analysis of Ojeda et al. (2021). We follow original morphological descriptions of the nominal forms (e.g. Cabrera, 1926; Crespo, 1964; Thomas, 1912, 1919) and revisionary studies of the genus *Phyllotis* (e.g. Hershkovitz, 1962; Pearson, 1958), to relate the characters' state observed in our samples with specimens of the several nominal forms described for the genus. When qualitative state characters were not useful (e.g. damaged or broken skulls and obliterated molars patterns), we followed a criterion of geographic proximity among localities (respect to the provenance localities of the sequenced specimens used in the phylogenetic analyses conducted by Ojeda et al., 2021 and to the collecting localities of confidently identified specimens). In using this last criterion, we took into account the presence of major geographic barriers between populations, environmental continuity and the absence of obvious discontinuities in size and shape of the skull (and in the external appearance of the skins) within groups (see Teta et al., 2018 and references there for a similar procedure).

2.4 | DNA Sequencing

We sequenced the partial or complete cytochrome b gene (*cytb*; 419 to 1,144 bp) for 47 individuals from localities of Mendoza and Neuquén provinces (Supplementary Material S1). These specimens were collected from an overlapping but more extensive range to that of *P.* sp. 2 in Ojeda et al. (2021). Amplifications and sequencing followed Steppan et al. (2007) using primers P484 and P485 for PCR with 35–40 cycles of 94°C (30–45 s), 55°C (45 s), and 72°C (90 s) between an initial denaturation at 94°C (2 min) and a terminal 72°C elongation (6–7 min). Sequences were aligned and individually checked for quality in Sequencher (GeneCodes Corp.)
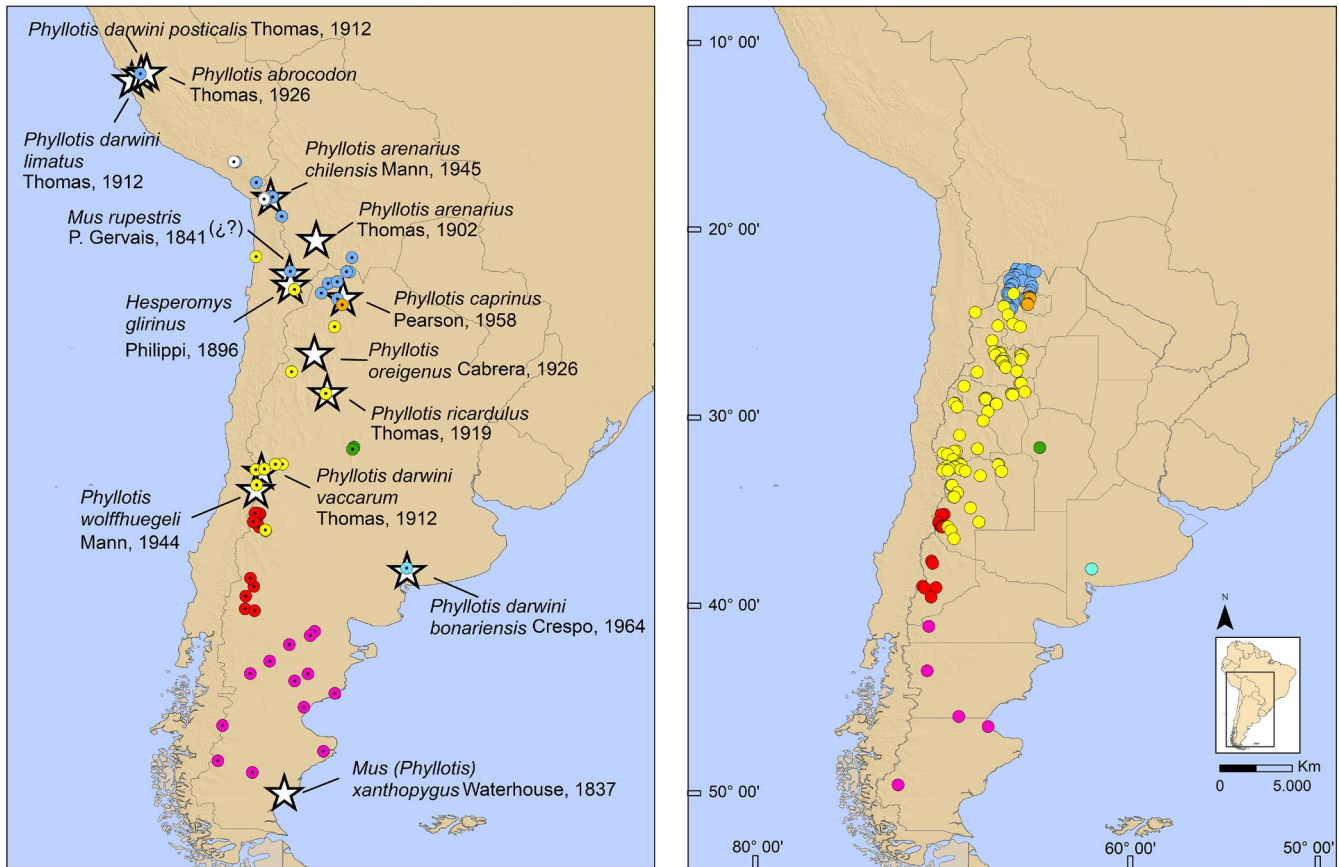
FIGURE 1 Maps showing type localities of the nominal forms related to the *P. xanthopygus* complex (stars) and the sequenced specimens included in Ojeda et al. (2021) (left), and the collecting localities of the specimens studied in the morphometric analyses (right). *Phyllotis bonariensis* (turquoise circles); *P. caprinus* (orange circles); clade of *P. x. posticalis-P. x. rupestris* (light blue circles); clade of *P.* sp. 1 (green circles); clade of *P.* sp. 2 (red circles); clade of *P. vaccarum* (yellow circles); clade of *P. xanthopygus* s.s. (pink circles)

and Mesquite v3.08 (Maddison & Maddison, 2017) before further analysis. Sequences have been deposited on Genbank with accession numbers MZ298848-MZ298894.

2.5 │ Phylogenetic analysis

The 47 new sequences for *cytb* were combined with 24 previously published sequences representing *P.* sp. 2, *P. bonariensis, P. caprinus, P. darwini, P. limatus, P. vaccarum, P. xanthopygus s.s., P. x. chilensis, P. x. posticalis* and *P. x. rupestris* for phylogenetic analysis. Sequences were aligned using Clustal Omega (Sievers et al., 2011), and optimization of phylogenetic inferences was performed by RAxML (Stamatakis, 2006), under the GTR+Γ substitution model selected by AIC in jModeltest2 (Darriba et al., 2012), using five batches of 100 searches, partitioned by codon position, and random seed values for initial trees. To infer support for clades, 1,000 bootstrap replicates were conducted. Patristic distances within and between clades for *cytb* were estimated in Mega X (Kumar et al., 2018).

2.6 │ Morphometric analyses

Standard external measurements were recorded from specimen labels or museum catalogs: total body length (including body plus tail length), TBL; tail length, T; hind foot length (including claw), HF; ear length, E; and weight, W. The following 24 skull measurements were recorded with digital calipers to the nearest of 0.01 mm following definitions provided by Hershkovitz (1962), Myers (1989) and Myers et al. (1990): total length of the skull, TLS; condyloincisive length, CIL; basal length, BL; palatal length, PL; diastema length, DL; palatal bridge, PB; maxillary toothrow length, MTRL; bullar length less tube, BLLT; bullar breadth, BuB; incisive foramina length, IFL; alveolar width 1 (across external side of both M1), AW1; alveolar width 2 (across external side of both M3), AW2; zygomatic length, ZL; zygomatic plate depth, ZP; zygomatic breadth, ZB; braincase breadth, BB; interorbital constriction, IOC; mid-rostral width, RW2; nasal length, NL; rostral length, RL; orbital length, OL; occipital condyle width, OCW. In addition, we recorded the following mandible

measurements: mandible length, ML; mandibular toothrow length, mTRL. A total of 604 specimens were assigned to five age classes (age class 1 = 188; age class 2 = 191; age class 3 = 129; age class 4 = 61; age class 5 = 35) based on tooth wear following the criteria figured and described by Jayat et al. (2016).

Descriptive morphometric and univariate comparisons (ANOVA several sample test and Tukey's pairwise comparison) for the specimens assigned to each one of the main clades recovered in the phylogenetic analysis developed by Ojeda et al. (2021) and for samples of each one of the nominal forms were carried out with the software PAST (Hammer et al., 2001). Specimens of age classes 2 and 3 were pooled (to obtain largest samples between available specimens) in tests of significant body and skull size differences (for both, $p \leq .05$ and $p \leq .01$).

In order to reduce the dimensionality of morphometric data and explore the differences in size of the skull among samples, we used a Principal Component Analysis (sPCA) for individuals in age classes 2 and 3. For this analysis, PCs were extracted from the variance–covariance matrix and computed by using variables after transformations to Log 10. We also conducted a Discriminant Function Analysis (sDFA) using the same set of specimens with the aim to evaluate significant differences among predefined groups and check for misclassified specimens. Subsequently, we explored differences in the shape of the skull among samples using a 'size-free' Principal Component Analysis (sfPCA) and a 'size-free' Discriminant Function Analysis (sfDFA), including all individuals without missing data (and pooling specimens of the five age classes). To reduce the effect of size, Mosimann shape variables were calculated through geometric mean transformation of data prior to statistical analyses (as developed by Meachen-Samuels & Van Valkenburgh, 2009). Statistical significance of the PCs were evaluated following the Broken-stick test (Frontier, 1976; Jackson, 1993). All multivariate statistical analyses, based on partial datasets (e.g. only specimens without missing values), were performed with the software PAST (Hammer et al., 2001).

To visualize geographic variation in the univariate space and search for clinical patterns or morphometric discontinuities within the clade of *P. vaccarum* of Ojeda et al. (2021), we constructed Dice-Leraas diagrams (modified from Hubbs & Hubbs, 1953) showing the median, the 25%–75% quartiles and the minimum and maximum values (calculated on the base of the geometric mean of each individual). We used specimens of age classes 2 and 3, including only those localities with more than 10 specimens (in some cases, we grouped geographically close localities to achieve this minimum sample size; see Libardi & Percequillo, 2016 for a similar analysis).

3 | RESULTS

3.1 | Taxonomic assignments

Populations of *Phyllotis* vary little in skull and molar morphology. Nonetheless, several qualitative characters allow us to allocate the specimens to each one of the four clades recovered by Ojeda et al. (2021) in the central Andes, from southwestern Bolivia to central western Argentina. Below we describe, from north to south, the morphological characteristics distinguishing each of these clades.

3.1.1 | The clade of *P. x. posticalis-P. x. rupestris*

We found qualitative morphological evidence for recognizing three taxa of the *P. xanthopygus* species complex that occur in sympatry in some localities, in the Puna and Altos Andes arid ecoregions of northwestern Argentina, in Jujuy and Salta provinces (Figure 1). One of these groups, assigned to the clade of *P. x. posticalis-P. x. rupestris* (Ojeda et al., 2021), is characterized by specimens with small and delicate skulls, with the interorbital region with rounded (not sharp-edged) borders, the frontoparietal suture mostly 'U' shaped, narrow rostrum (Figure 2), and by a simplified enamel molar patterns on the upper molar series, which are characterized by a very shallow paraflexus on M2 and no trace of the mesoloph complex (sensu Barbière et al., 2019) on M1 and M2 (Figure 3).

The clade of P. caprinus.

Other specimens registered in the extreme north of our study area (Figure 1) show morphological state characters that closely match to those described for *P. caprinus*. Specimens assigned to this clade have large and heavy skulls, with a flat, sharp-edged, long-waisted interorbital region, a predominantly 'V' shaped frontoparietal suture and a comparatively heavy rostrum (Figure 2). All specimens assigned to this clade come from the type locality of *P. caprinus* or nearby areas in Jujuy Province (Figure 1).
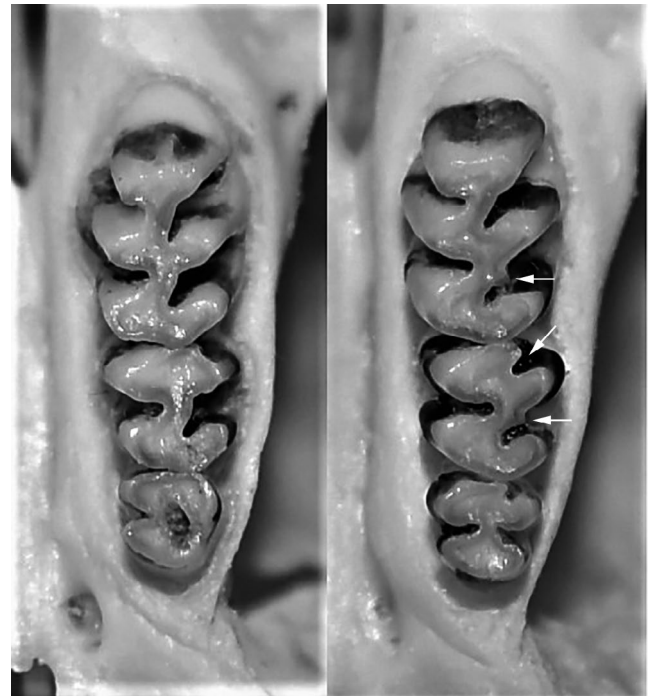
The clade of P. vaccarum.

From the western limit between Jujuy and Salta provinces to southern Mendoza Province (Figure 1), we found qualitative and quantitative morphologic characters for recognizing two other taxa of the *P. xanthopygus* complex. One of them corresponds to individuals that are representative of the clade of *P. vaccarum* (Ojeda et al., 2021), which is sympatric, in the arid cold Puna ecoregion of southwestern Jujuy and northwestern Salta provinces, with specimens corresponding to the form here referred to *P. x. posticalis-P. x. rupestris* (Ojeda et al., 2021, Figure 1). Populations assigned to the clade of *P. vaccarum* differ from those of the clade of *P. x. posticalis-P. x. rupestris* by having larger and

FIGURE 2 Dorsal view of the skull showing some morphological character states differentiating specimens of the clade of *P. x. posticalis-P. x. rupestris* (left: MACN-Ma 29596) and *P. caprinus* (right: MACN-Ma 29425) in northwestern Argentina. Notice the smaller and more delicate skulls, the rounded (not sharp-edged) interorbital region, the frontoparietal suture mostly 'U' shaped and the narrow rostrum in the specimen of *P. x. posticalis-P. x. rupestris*. Scale bar = 10 mm

FIGURE 3 Occlusal molar view showing the simplified enamel molar pattern (very shallow or absent paraflexus on M2 and no trace of mesoloph complex on M1 and M2) on the upper molar series of specimens of the clade of *P. x. posticalis-P. x. rupestris* (left: MACN-Ma 29594), in comparison with the more complex pattern generally observed in specimens of the clade of *P. vaccarum* (right: MACN-Ma 29565). Photographs are not in scale

heavier skulls, more robust molar series, and more complex enamel molar patterns, which are characterized by a generally very deep paraflexus on M2 and by the presence of a poorly developed but clearly visible mesoloph complex on M1 and M2 (Figure 3). This clade is morphologically cohesive and encompasses several of the nominal forms described for the region (i.e. *oreigenus* with type locality in Laguna Blanca, north-central Catamarca Province; *ricardulus* with type locality in Otro Cerro, southern Catamarca Province; and *darwini vaccarum* with type locality in Punta de Vacas, northwestern Mendoza Province). We examined type, paratypes or topotypes of all these nominal forms and several geographic intermediate populations from western Argentina (in La Rioja, Salta, San Juan, San Luis, and Tucumán provinces) and did not find constant qualitative morphologic differences in the skull and enamel molars patterns to distinguish among them (Figures 4 and 5). In southwestern Mendoza and northwestern Neuquén provinces (Figure 1), representatives of the clade of *P. vaccarum* are sympatric with populations corresponding to the clade of *P. sp. 2* (Ojeda et al., 2021), which represent an undescribed species that will be treated in depth in following paragraphs and in the discussion section of this study. Cytb sequence data indicate that the clade of *P. vaccarum* extends further

to the west in the higher elevations of Chile (Steppan & Ramírez, 2015; Storz et al., 2020).

3.1.2 | The clade of *P.* sp. 2

We recorded specimens of this clade in sympatry (and in syntopy), in at least one locality, with populations of the clade of *P. vaccarum* in southwestern Mendoza Province (Figure 1). The skulls of specimens of both clades are very similar, but the molars in *P.* sp. 2 are appreciably less robust and show a more simplified enamel molar pattern, without the deep paraflexus on M2 and the mesoloph complex on M1 and/or M2 observed in specimens of the clade of *P. vaccarum* (Figure 6). We also observed some integumental characters (see the discussion section) that differentiate both taxa and facilitate the assignment of these specimens in sympatric areas.

DNA samples from throughout the range of *P.* sp. 2, as delimited by the morphological characters, and sequenced for *cytb* to test the species limits, greatly expanded the range for DNA data beyond that in Ojeda et al. (2021). The phylogeny (Figure 7) clearly corroborates the prior results, with the 47 new sequences from all 10 localities assigned
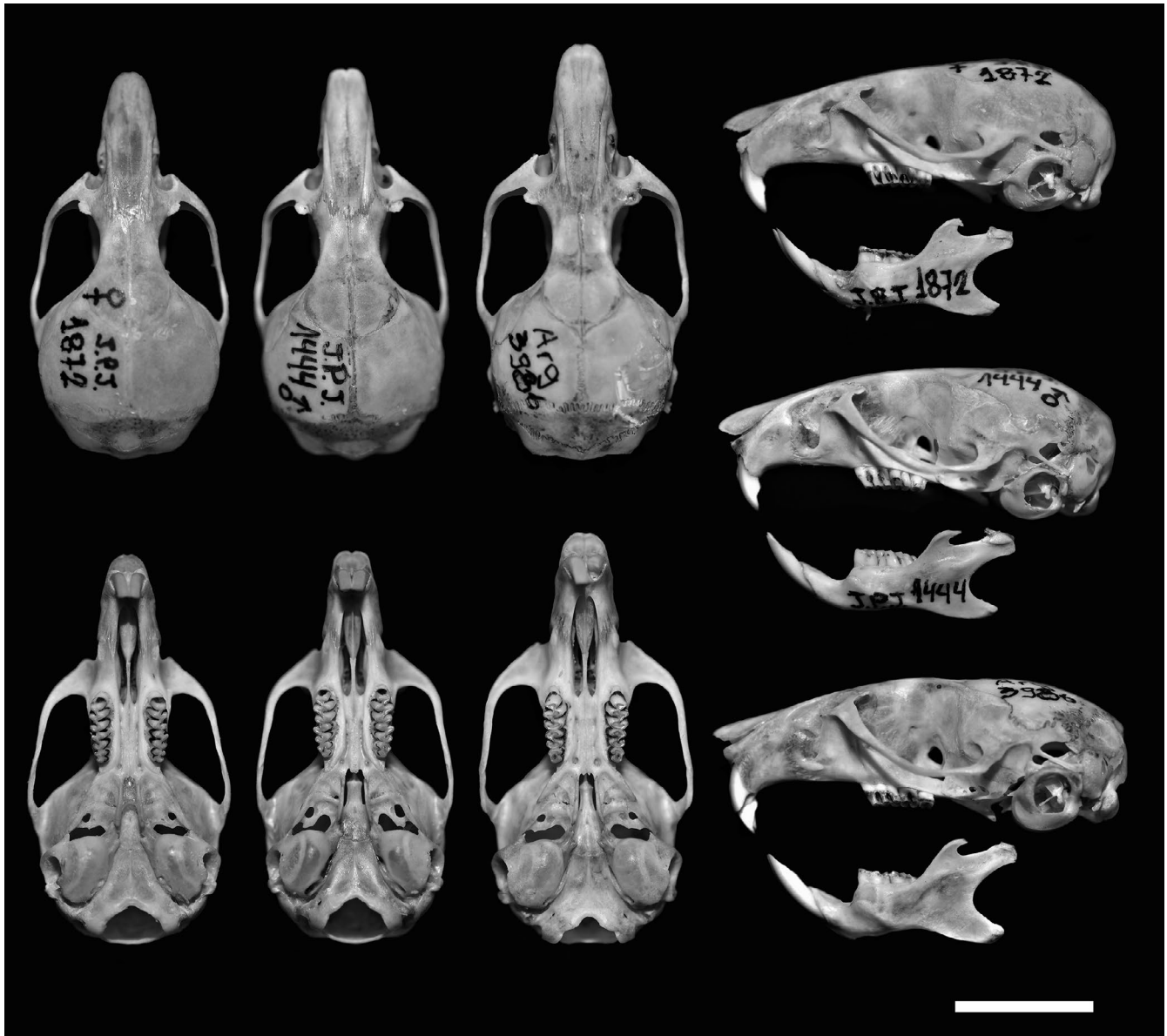
FIGURE 4 Dorsal, ventral and lateral view of the skull, and lateral view of the mandible of topotype specimens of the nominal forms *Phyllotis oreigenus* (left and top: MACN-Ma 29565), *P. ricardulus* (centre: MACN-Ma 29605) and *P. darwini vaccarum* (right and bottom: CML 4480). Scale bar = 10 mm

to *P.* sp. 2 by morphology forming a well-differentiated mitochondrial clade along with the eight sequences from the four localities from Ojeda et al. (2021). Genetic distances (p) ranged from 0% to 3.5% within the clade of *P.* sp. 2 with a mean of 1.5%, and 8.8%–11.5% among members of this clade and the other taxa of the *P. xanthopygus* complex discussed here.

3.2 | Morphometric analyses

Descriptive morphometrics comparing five of the eight main clades obtained by Ojeda et al. (2021) are summarized in Table 1. The ANOVA showed a good separation among

populations representing each clade for all the metric state characters analysed (Supplementary Material S2). Tukey's pairwise comparisons indicated one external (W) and several skull (e.g. TSL, CIL, MTRL, BLLT, BuB, IFL, AW1, AW2, ZL, ZB, mTRL) measurements that significantly differed among most of these main clades (Supplementary Material S2).

Specimens of the clade of *P. x. posticalis-P. x. rupestris* were the smallest among the studied samples. This holds for all the studied characters with only two exceptions, BLLT and the BuB, which averaged larger in this sample compared with *P. caprinus* (Table 1). This clade differed in 14 or more characters when compared with populations of the other clades (Supplementary Material S2).

FIGURE 5 Occlusal molar view showing the enamel molar pattern (well-developed paraflexus on M2 and visible mesoloph complex on M1 and M2) on the upper molar series of specimens of the nominal forms *Phyllotis oreigenus* (left: MACN-Ma 29565), *P. ricardulus* (centre: MACN-Ma 29601) and *P. darwini vaccarum* (right: CML 4478)

FIGURE 6 Occlusal molar view showing the simplified enamel molar pattern (very shallow or absent paraflexus on M2 and no trace of mesoloph complex on M1 and M2) on the upper molar series of specimens of the clade of *P.* sp. 2 (left: CMI 7638), in comparison with the more complex pattern generally observed in specimens of the clade of *P. vaccarum* (right: MACN-Ma 29565). Photographs are not in scale

Samples representatives of *P. caprinus* were intermediate in size, showing several morphometric state characters significantly differing from *P. bonariensis*, the clade of *P.* sp. 2., and the clade of *P. x. posticalis-P. x. rupestris* (Supplementary

Material S2). This species was morphometrically very similar to samples of specimens of the clade of *P. vaccarum*, but they differed in four measurements (Supplementary Material S2). *Phyllotis caprinus* shows, in average, the smaller ears (E) and bullar measurements (both, BLLT and BuB), but the broader interorbital constriction (IOC) of all the studied samples (Table 1).

With the exception of *P. caprinus*, samples of the clade of *P. vaccarum* clearly separate from other clades. Specimens of this clade were intermediate in size (smaller than *P. bonariensis* and the clade of *P.* sp. 2 and larger than the clade of *P. x. posticalis-P. x. rupestris*) (Table 1), differing by 20 or more morphometric state characters when compared with the other clades (Supplementary Material S2). Univariate statistical analyses showed scarce differentiation among the nominal forms included within this clade (Supplementary Material S3). Only the nominal form *ricardulus* could be somewhat separated from the nominal forms *oreigenus* and *vaccarum* (and from populations representing the entire geographic range of the clade of *P. vaccarum* in western Argentina). This nominal form averaged significantly smaller than samples of the clade of *P. vaccarum* (in nine skull measurements), and topotype specimens of the *oreigenus* (eight skull measurements) and the *vaccarum* (one external and six skull measurements) nominal forms.

Samples of specimens here assigned to the clade of *P.* sp. 2 were comparatively large sized, averaging larger for most measurement when compared with all clades excepting *P. bonariensis* (Table 1). This last species was the most similar, but it averaged significantly larger for 13 measurements, including both measurements of the length (e.g. TLS, CIL, PL, DL, PB) and the width (e.g. AW1, ZB, IOC, RW2, OCW) of the skull (Supplementary Material S2).

FIGURE 7 Maximum likelihood phylogeny of *cytb* sequences including all new and published samples for *P*. sp. 2 and a representative sampling for other taxa in the *Phyllotis xanthopygus* species complex. Individuals are identified by Genbank accession number or for newly sequenced individuals, by the collector's number (see Supplementary Material S1). Localities are indicated in (parentheses), corresponding to those listed in the Specimens Examined (Supplementary Material S1). Numbers above nodes are bootstrap percentages for values >50%. Scale bar is expected substitution rate

0.03
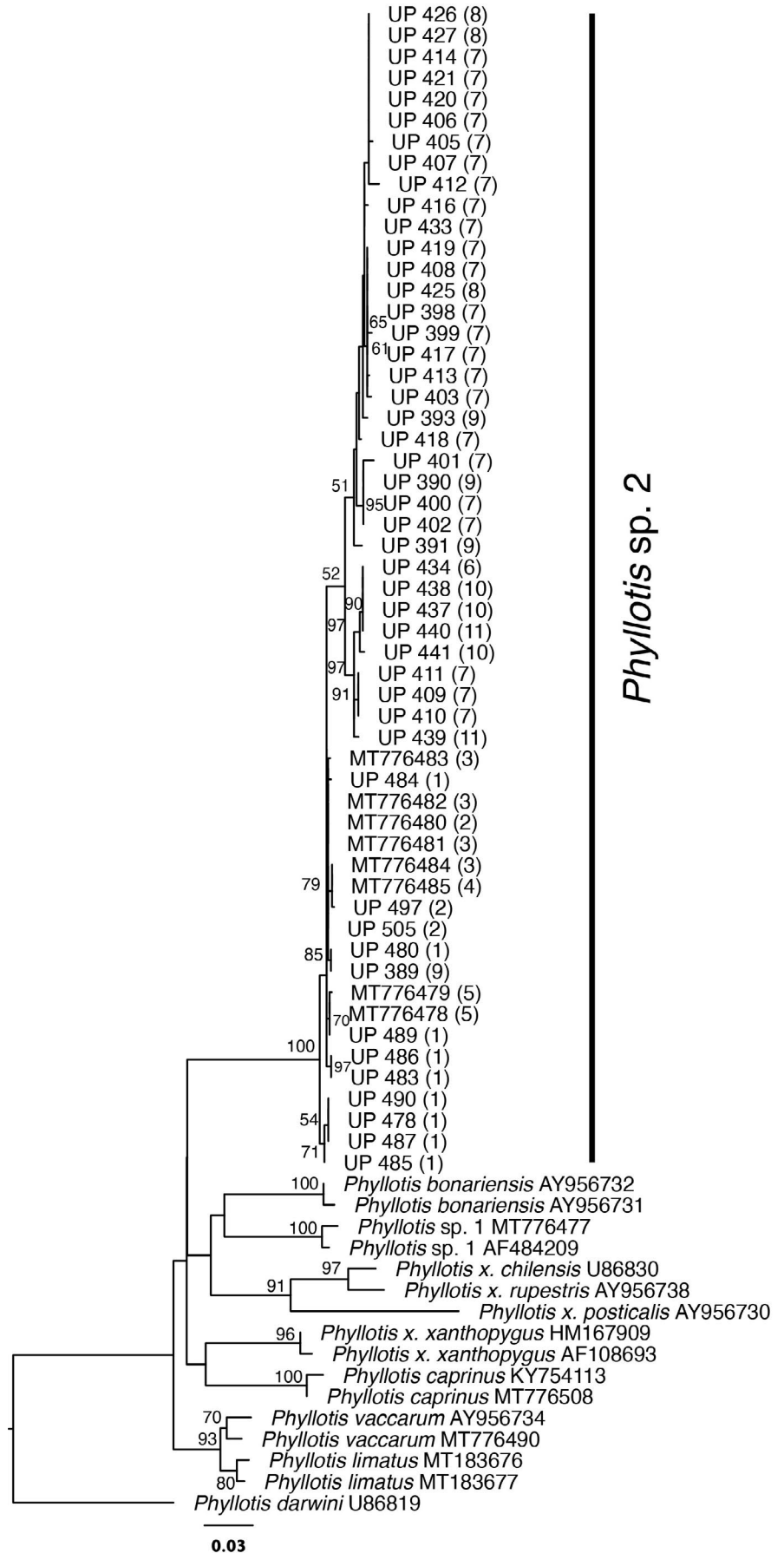
TABLE 1 External and craniodental measurements for specimens (age classes 2 and 3) of five of the eight main clades obtained by Ojeda et al. (2021) for the *Phyllotis xanthopygus* complex

	P. bonariensis			*P. caprinus*			*P. x. posticalis-P. x. rupestris*			*P. vaccarum*			*P. sp. 2*		
	n	X ± SD	r	n	X ± SD	r	n	X ± SD	r	n	X ± SD	r	n	X ± SD	r
TBL	5	255 ± 9.37	240–262	8	225 ± 16.40	202–245	57	224 ± 18.07	129–253	92	235 ± 22.48	120–274	14	240 ± 15.14	216–280
T	5	124 ± 9.97	110–135	8	118 ± 16.22	82–133	57	114 ± 8.33	95–129	92	120 ± 13.50	80–152	14	115 ± 7.43	102–135
HF	5	27 ± 1.14	25–28	11	27 ± 2.31	21–29	56	25 ± 1.62	19–29	94	28 ± 1.68	23–32	15	30 ± 2.50	25–33
E	5	24 ± 0.71	23–25	11	22 ± 1.42	19–24	56	25 ± 1.87	20–30	94	25 ± 1.61	21–30	15	25 ± 1.45	22–27
W	5	72 ± 12.58	62–87	9	38 ± 10.78	22–59	49	41 ± 7.64	25–55	83	47 ± 11.02	27–79	14	55 ± 14.29	36–80
TLS	6	33.04 ± 1.38	31.74–35.24	11	30.47 ± 1.91	28.00–34.68	65	28.93 ± 1.97	26.51–30.99	99	30.02 ± 1.20	27.26–32.70	15	31.43 ± 0.94	30.29–33.56
CIL	6	30.95 ± 1.55	29.35–33.61	13	27.70 ± 2.01	24.06–31.92	66	26.54 ± 1.03	23.83–28.73	101	27.78 ± 1.30	24.82–30.70	15	28.88 ± 0.93	27.77–30.97
BL	6	28.52 ± 1.49	26.98–31.20	13	25.23 ± 2.03	21.61–29.56	64	24.43 ± 1.03	21.62–26.43	101	25.50 ± 1.28	22.82–28.89	15	26.62 ± 0.81	25.39–28.31
PL	6	17.47 ± 0.64	16.87–18.44	14	15.27 ± 0.95	13.23–17.24	68	14.75 ± 0.58	13.44–15.93	101	15.64 ± 0.74	13.97–17.38	16	16.30 ± 0.53	15.58–17.35
DL	6	8.86 ± 0.49	8.33–9.71	15	7.62 ± 0.65	6.18–8.84	69	7.42 ± 0.39	6.37–8.20	102	7.69 ± 0.45	6.65–8.83	16	8.08 ± 0.47	7.57–8.99
PB	6	6.44 ± 0.29	6.12–6.82	14	5.42 ± 0.29	4.97–5.92	68	5.22 ± 0.29	4.35–6.26	101	5.62 ± 0.36	4.63–6.61	16	5.76 ± 0.28	5.14–6.29
MTRL	6	5.97 ± 0.25	5.57–6.20	15	5.27 ± 0.26	4.85–5.76	70	5.00 ± 0.16	4.59–5.30	103	5.42 ± 0.28	4.81–6.16	16	5.85 ± 0.19	5.59–6.20
BLLT	6	5.96 ± 0.34	5.42–6.32	12	5.15 ± 0.34	4.60–5.73	68	5.41 ± 0.26	4.58–6.00	101	5.59 ± 0.35	4.91–6.32	15	6.10 ± 0.24	5.67–6.51
BuB	6	5.08 ± 0.22	4.67–5.28	12	4.33 ± 0.34	3.70–4.84	68	4.72 ± 0.16	4.44–5.15	101	4.90 ± 0.24	4.26–5.39	15	5.24 ± 0.19	4.86–5.57
IFL	6	7.99 ± 0.53	7.20–8.77	15	6.99 ± 0.54	5.80–8.03	69	6.84 ± 0.42	5.34–7.63	102	7.07 ± 0.46	5.92–8.19	16	7.41 ± 0.31	6.99–8.20
AW1	6	6.25 ± 0.30	5.94–6.62	15	5.73 ± 0.17	5.39–6.07	68	5.73 ± 0.16	5.33–6.10	103	5.81 ± 0.22	5.32–6.37	16	5.95 ± 0.20	5.55–6.32
AW2	6	5.68 ± 0.19	5.35–5.86	15	5.18 ± 0.25	4.76–5.57	68	5.00 ± 0.18	4.59–5.31	103	5.24 ± 0.25	4.76–5.79	16	5.43 ± 0.23	5.09–5.84
ZL	6	17.06 ± 0.78	16.03–18.38	15	15.80 ± 0.82	14.45–17.35	68	14.95 ± 0.60	13.26–16.15	103	15.73 ± 0.72	14.18–17.68	16	16.56 ± 0.59	15.67–17.49
ZP	6	3.75 ± 0.14	3.60–3.97	15	3.34 ± 0.27	2.78–3.74	70	3.26 ± 0.25	2.51–3.72	103	3.41 ± 0.27	2.79–4.13	16	3.59 ± 0.18	3.20–3.87
ZB	6	17.18 ± 0.76	16.50–18.50	14	15.44 ± 0.78	14.06–16.92	66	14.83 ± 0.54	13.38–16.15	103	15.54 ± 0.61	14.20–16.78	16	15.99 ± 0.48	15.01–16.54
BB	6	14.38 ± 0.33	13.85–14.74	15	13.52 ± 0.40	12.88–14.26	68	13.31 ± 0.34	12.65–14.23	102	13.70 ± 0.36	12.81–14.46	15	13.94 ± 0.31	13.41–14.46
IOC	6	4.44 ± 0.19	4.18–4.69	15	4.53 ± 0.29	4.22–5.19	69	4.16 ± 0.15	3.85–4.59	103	4.31 ± 0.19	3.92–4.82	16	4.14 ± 0.18	3.85–4.44
RW2	6	5.95 ± 0.33	5.58–6.48	15	5.06 ± 0.40	4.18–5.91	68	4.88 ± 0.30	4.25–5.55	103	5.01 ± 0.28	4.43–5.72	16	5.10 ± 0.28	4.67–5.63
NL	6	14.45 ± 0.61	13.38–15.10	13	12.79 ± 0.72	11.68–14.07	68	12.4 ± 0.60	10.76–13.85	101	12.64 ± 0.75	11.03–14.59	16	13.77 ± 0.56	12.96–14.75
RL	6	12.96 ± 0.53	12.58–13.88	13	11.64 ± 0.77	10.41–13.44	68	11.10 ± 0.48	10.10–12.45	101	11.56 ± 0.66	10.15–13.09	16	12.30 ± 0.47	11.67–13.33
OL	6	11.21 ± 0.41	10.70–11.80	15	10.14 ± 0.60	9.23–11.17	69	9.50 ± 0.42	8.27–10.39	103	10.19 ± 0.41	9.02–11.17	16	10.74 ± 0.38	10.26–11.42
OCW	6	7.40 ± 0.21	7.12–7.66	13	7.09 ± 0.19	6.78–7.46	65	6.75 ± 0.20	6.28–7.25	102	7.08 ± 0.24	6.60–7.78	15	7.07 ± 0.20	6.79–7.39
ML	6	17.51 ± 0.82	16.33–18.72	15	15.59 ± 0.91	14.23–17.50	68	15.22 ± 0.53	13.90–16.32	103	15.98 ± 0.73	14.23–17.89	16	16.92 ± 0.62	16.15–18.54
mTRL	6	5.90 ± 0.16	5.74–6.10	15	5.34 ± 0.27	5.00–5.91	69	5.03 ± 0.18	4.63–5.38	103	5.36 ± 0.23	4.78–5.96	16	5.77 ± 0.16	5.44–5.96

Note: Measurement abbreviations are listed in Materials and Methods.

Abbreviations: *n*, sample size; *r*, range; *SD*, standard deviation; X, mean.

The first 3 principal components of the sPCA accounted for 76.55% of the variability in the data set, but only the first (64.21% of the variance explained) was judged statistically significant by the Broken-stick test (Table 2). PC I was a size component, as all the variables had equal sign and loaded heavily on this axis (we confirm this by regressing PC I scores against several total length measures). This PC mainly separated samples of the small-sized *P. x. posticalis-P. x. rupestris* on the negative side, from the larger *P.* sp. 2 (and *P. bonariensis*) located well on the positive side. Samples of *P. caprinus* and specimens representing the clade of *P. vaccarum* occupied an intermediate position, widely overlapping on this PC with other samples (excepting *P. bonariensis*) (Figure 8). PC II mostly separated specimens of *P. caprinus* (well on the negative side), from the samples

of the *P. x. posticalis-P. x. rupestris*, the *P. vaccarum*, and the *P.* sp. 2 clades, mainly by metric characters related to the bulla (BLLT and BuB), the molar row series (MTRL and mTRL) and the rostrum (RW2) (Table 2 and Figure 8). *Phyllotis caprinus* shows smaller bullae and molar series but a broader rostrum. In summary, the bivariate plot of PC I and PC II shows a good separation among samples of all studied clades with the only exception of *P. vaccarum*, which is more variable and widely overlaps with specimens of the *P. x. posticalis-P. x. rupestris* and the *P.* sp. 2 clades (Figure 8).

The sDFA (Table 2) completely separated the samples of *P. x. posticalis-P. x. rupestris*, *P. caprinus*, *P.* sp. 2 and *P. bonariensis*. Specimens of the clade of *P. vaccarum* slightly overlapped with those of *P. caprinus* and *P. x. posticalis-P. x. rupestris*, but heavily overlapped with samples

TABLE 2 Results of the sPCA and sDFA comparing five of the eight main clades obtained by Ojeda et al. (2021) for the *Phyllotis xanthopygus* complex

| Variables | Eigenvectors | | | Eigenvectors | | | |
	PC 1*	PC 2	PC 3	DF 1	DF 2	DF 3	DF 4
TLS	0.20189	−0.091675	0.018215	0.006791	−0.00080839	0.0073229	0.00065257
CIL	0.22862	−0.11153	0.021123	0.0076825	−0.0011583	0.007479	−0.0014684
BL	0.23718	−0.10804	−0.017943	0.0075585	−0.000164	0.0081219	−0.001697
PL	0.24086	−0.060011	0.07054	0.0091748	−0.00032107	0.0068221	−0.0030643
DL	0.25007	−0.26457	−0.11006	0.0070834	−0.0001997	0.010655	−0.0033772
PB	0.23512	0.14808	0.44351	0.011039	−0.00049466	0.0069655	−0.0085175
MTRL	0.22986	0.38844	0.23825	0.012853	0.002658	0.0061106	0.0010651
BLLT	0.18466	0.42653	−0.45067	0.0072513	0.0092084	0.0065521	0.0013531
BuB	0.17913	0.3782	−0.24409	0.0073746	0.011615	0.002334	−0.0037874
IFL	0.24283	−0.26767	−0.25328	0.0064484	0.0009399	0.0099851	−0.0016779
AW1	0.093554	−0.018907	0.035335	0.0030208	5.39E−01	0.0053949	−0.0023438
AW2	0.15597	0.17874	0.082756	0.0074285	−0.0005764	0.0047833	−0.0017979
ZL	0.21383	0.02365	−0.025498	0.0080517	1.89E−01	0.005583	0.00071986
ZP	0.26197	−0.024232	−0.22837	0.0075098	0.0035559	0.0069328	−0.0030443
ZB	0.18422	−0.051331	0.099502	0.007143	−0.00086808	0.0062946	−0.0034899
BB	0.095676	0.044527	0.080576	0.004472	0.00026256	0.0027563	−0.0018798
IOC	0.038667	−0.1387	0.39915	0.0032077	−0.0076132	−0.0014234	−0.0045258
RW2	0.20408	−0.39312	0.05642	0.0047758	−0.0038956	0.01309	−0.0059822
NL	0.23231	−0.11651	−0.21014	0.0060147	0.0023477	0.013055	0.0029131
RL	0.24461	−0.071999	−0.067777	0.0076722	0.0002206	0.0092537	0.00065939
OL	0.22583	−0.032701	0.14077	0.010559	−0.00072364	0.0056227	−0.00027935
OCW	0.10848	0.024653	0.21529	0.0059913	−0.0023479	0.00071538	−0.0033741
ML	0.22335	0.0079482	0.0024213	0.0085466	0.0018427	0.0064958	−1.06E−01
mTRL	0.1918	0.3035	0.2163	0.010947	0.00097811	0.0069765	0.0030469
Eigenvalue	0.00982538	0.00104763	0.000839976	2.6777	1.1085	0.73487	0.40623
% variance	64.21	6.85	5.49	54.34	22.50	14.91	8.244

Note: Phyllotis bonariensis (N = 6), *P. caprinus* (N = 8), clade of *P. x. posticalis-P. x. rupestris* (N = 59), clade of *P.* sp. 2 (N = 15) and clade of *P. vaccarum* (N = 97). Loadings of the variables, eigenvalues and proportion of the variance explained for the first 3 principal components (PC) and the first 4 discriminant functions (DF). Results are based on log10-transformed craniodental variables. See 'Material and Methods' for variable abbreviations.
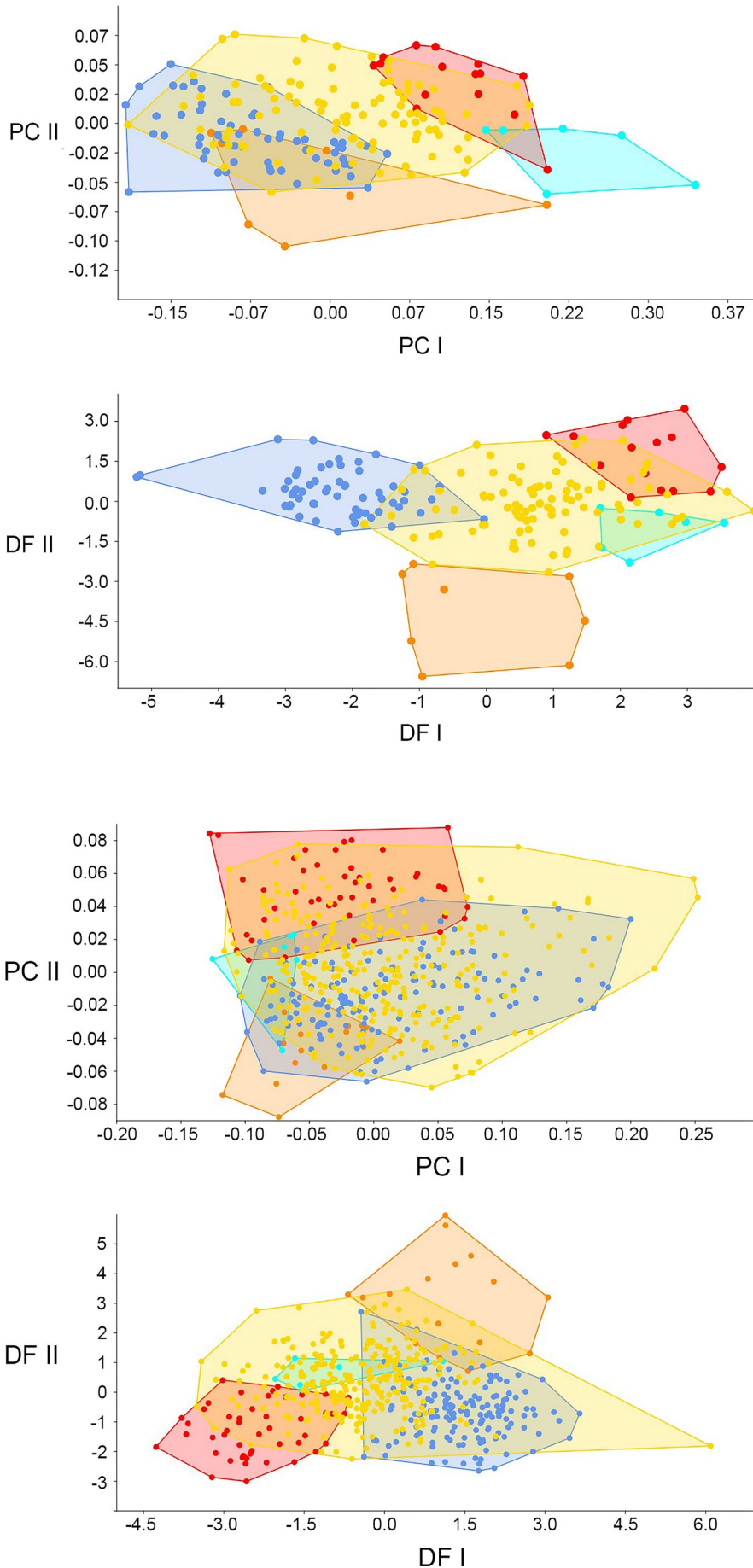
FIGURE 8 Individual specimen scores based on log-transformed values of 24 cranial measurements projected onto the first and second principal components of the sPCA (top), and the first and second discriminant functions (DF) of the sDFA (bottom) extracted from analysis of specimens (age classes 2 and 3) of *Phyllotis bonariensis* (turquoise dots, *N* = 6), *P. caprinus* (orange dots, *N* = 8), clade of *P. x. posticalis-P. x. rupestris* (light blue dots, *N* = 59), clade of *P.* sp. 2 (red dots, *N* = 15) and clade of *P. vaccarum* (yellow dots, *N* = 97). Character loadings and the variance explained by each of the first three principal components and each of the four discriminant functions appear in Table 2

FIGURE 9 Individual specimen scores based on log-transformed values of 24 cranial measurements (Mosimann shape variables) projected onto the first and second principal components of the sfPCA (top) and the first and second discriminant functions (DF) of the sfDFA (bottom) extracted from analysis of specimens (all age classes) of *Phyllotis bonariensis* (turquoise dots, *N* = 6), *P. caprinus* (orange dots, *N* = 16), clade of *P. x. posticalis-P. x. rupestris* (light blue dots, *N* = 155), clade of *P.* sp. 2 (red dots, *N* = 47) and clade of *P. vaccarum* (yellow dots, *N* = 283). Character loadings and the variance explained by each of the first three principal components and each of the four discriminant functions appear in Table 3

referred to the clade of *P*. sp. 2 and *P. bonariensis* (Figure 8). DF I (54.34% of the variance explained) segregated the samples mostly by the molar tooth rows (upper and lower), the orbital length (OL) and the palatal bridge (PB). The DF II also separated well *P. caprinus* (on the negative side) from the other samples. Metric characters related to the bulla, the rostrum and the interorbital region were the most influential (Table 2). The percentage of correct classifications following the jackknifed confusion matrix of this analysis was 80.54% (Supplementary Material S4). Most of the specimens of the clades of *P. x. posticalis-P. x. rupestris* (93%), *P*. sp. 2 (93%), *P. vaccarum* (72%) and *P. bonariensis* (83%) were correctly classified, but *P. caprinus* obtained intermediate values (63%).

The sfPCA showed a large overlap for most of the studied samples, but specimens corresponding to *P. caprinus* (lower left quadrant) and the clade of *P*. sp. 2 (upper left quadrant) appeared as well separated each other on the bivariate plot of PC I and PC II (Figure 9). This separation was mostly influenced by the molar series (MTRL and mTRL) and the bullae (BLLT and BuB), which were larger in *P*. sp. 2, and the interorbital constriction (IOC) and the mid-rostral width, which were wider in *P. caprinus* (Table 3). The first principal component (the only judged statistically significant according to the Broken Stick test) of this analysis summarized 44.71% of the explained variance.

Similar results to that showed by the sfPCA were obtained with the sfDFA analysis, but in this case *P. caprinus* separated much better from *P*. sp. 2 (specimens of *P. caprinus* occupy mostly the right upper quadrat and those of the clade of *P*. sp. 2 the left lower quadrat, of the multivariate space) and the rest of the samples, which overlapped heavily (Figure 9). This analysis also revealed the influence of the metric characters related to the bulla, the molar series and the interorbital region as determinant for the separation of *P. caprinus* (which showed the smallest bullae and molar series, and the broadest interorbital constriction revealed by previous analyses; Table 3). The percentage of correct classifications following the jackknifed confusion matrix of the sfPCA was 73.37% (Supplementary Material S4). Most of the specimens of the clades of *P. x. posticalis-P. x. rupestris* (86%), *P*. sp. 2 (83%) and *P. bonariensis* (83%) were correctly classified, but the other samples obtained intermediate values (65% for the clade of *P. vaccarum* and 63% for *P. caprinus*).

4 | DISCUSSION

4.1 | Species limits in the *P. xanthopygus* species complex of the central Andes

The morphometric similarity (size and shape of the skull) in populations of the *P. xanthopygus* species complex has been already documented (e.g. Pearson, 1958; Steppan, 1998; Teta et al., 2018). At least in part, this morphological homogeneity explains the assignment of most of these populations (i.e. nominal forms) to the several subspecies of *P. xanthopygus* s.l. In this work, we also documented those morphometric similarities for the populations of the central Andes. Despite strong genetic divergences that indicate a significant period of isolation and divergence (having been suggested began between 2.83 and 4.05 MA AP in the Pliocene; Riverón, 2011), this low morphological variability could be explained by strong stabilizing selection favouring niche conservatism and phenotypic stasis, resulting in cryptic species. Nonetheless, there are some differences in size and shape of the skull that may be appropriate to establish morphometric limits. In the following paragraphs we discuss these morphometric differences and other sources of evidence (qualitative morphology of the skull and molars, cytogenetic data and geographic distribution patterns), which could be viewed as indicators of the specific status of these forms in light of the mitochondrial phylogeny.

4.2 | The clade of *P. x. posticalis-P. x. rupestris*

According to the phylogenetic analyses of Ojeda et al. (2021; see also Albright, 2004 and Steppan et al., 2007), representatives of this clade in northwestern Argentina correspond to a southern sub-clade widely distributed from west-central Bolivia to extreme northwestern Argentina. We did not measure specimens of this clade from Bolivia or Peru, precluding us from resolving the status of Argentinean populations; nevertheless, we are confident that Argentinean specimens represent a morphological cohesive sample and a different species from other clades of the eastern Andean flanks of western Argentina. Mean pairwise genetic distances between *P. x. posticalis-P. x. rupestris* and other clades of the *P. xanthopygus* complex range from 9.3% to 10.6% (see Table 1 in Ojeda et al., 2021), coinciding with (or well above of) the values observed among other species of *Phyllotis* (e.g. Jayat et al., 2016; Ojeda et al., 2021; Rengifo & Pacheco, 2017). Specimens of this clade from Jujuy Province show chromosome complements with 2n = 38, FNa = 70–71, including acrocentric autosomes with different patterns of heterochromatin, which are not present in samples from Catamarca and northern Mendoza here assigned to the clade of *P. vaccarum* (with 2n = 38, FNa =72 and a karyotype with all biarmed chromosomes and lower amount of heterochromatin). Specimens of *P*. sp. 2 have 2n = 38, FNa = 71–72 and present more heterochromatin than members of the clade of *P. x. posticalis-P. x. rupestris*, including an exclusive acrocentric autosome mostly heterochromatic (Labaroni et al., 2014). Furthermore, our morphometric

TABLE 3 Results of the sfPCA and sfDFA comparing five of the eight main clades obtained by Ojeda et al. (2021) for the *Phyllotis xanthopygus* complex

Variables	Eigenvectors			Eigenvectors			
	PC 1*	PC 2	PC 3	DF 1	DF 2	DF 3	DF 4
TLS	−0.064486	−0.00081786	0.09055	0.0005501	0.0014951	−0.0025847	−0.0018964
CIL	−0.14443	−0.014142	0.10604	−0.00033915	0.0030881	−0.0031464	0.00019611
BL	−0.17718	0.00015537	0.089086	−0.00036487	0.0020992	−0.0038998	0.00061931
PL	−0.14729	0.054239	0.16222	−0.0023649	0.0024609	−0.000774	0.0021849
DL	−0.28704	−0.087896	0.079574	0.00080222	0.0023844	−0.0054639	0.0050455
PB	0.032972	0.13568	0.45638	−0.003321	0.0029763	0.0035788	0.0072166
MTRL	0.21893	0.39578	0.10228	−0.0077591	−0.0022133	0.0020275	−0.0023089
BLLT	0.17843	0.3551	−0.5252	−0.00054067	−0.010588	0.0036351	−0.0024004
BuB	0.19548	0.24465	−0.28461	−0.0014576	−0.0096625	0.010565	−0.0011718
IFL	−0.2404	0.022381	0.0039828	−0.00073701	0.0012578	−0.0039838	0.0022323
AW1	0.20388	−0.22688	−0.16201	0.0071951	−0.0028616	0.0043505	0.00060222
AW2	0.15842	−0.14289	−0.14568	0.0022153	−0.00090324	0.0022975	0.0005136
ZL	−0.077017	−0.00257	−0.02344	−0.00028538	0.0022044	−0.00023174	−0.0018018
ZP	−0.35194	−0.18375	−0.49253	−0.0020028	−0.001167	−0.0060887	−0.0013915
ZB	0.0080186	−0.098001	0.033125	0.001098	0.0012575	−7.54E−05	0.0010577
BB	0.24481	−0.13611	−0.01532	0.0047537	−0.0017854	0.0063639	−0.002689
IOC	0.40055	−0.49845	0.088899	0.0094794	0.0054394	0.0094494	−0.0034131
RW2	−0.1057	−0.30612	−0.049949	0.0029669	0.0020517	−0.0067643	0.0071927
NL	−0.2201	0.11725	−0.03161	−4.89E−05	−0.0027306	−0.010025	−0.000524
RL	−0.21935	0.1219	0.063147	−0.0021651	0.0006078	−0.006809	−0.0010116
OL	−0.037728	0.019585	0.16407	−0.0038804	0.0037381	0.00080492	−0.00018664
OCW	0.25364	−0.13822	0.1041	0.0032537	0.0029731	0.0083603	−0.0027789
ML	−0.079334	0.051403	0.063133	−0.0021905	−0.00022496	−0.0023266	−0.0022353
mTRL	0.25686	0.31782	0.12376	−0.0048572	−0.0018976	0.00073995	−0.0030516
Eigenvalue	0.0041704	0.00104178	0.00070736	1.3505	0.66717	0.31121	0.13745
% variance	44.71	11.17	7.58	54.76	27.05	12.62	5.57

Note: Phyllotis bonariensis (N = 6), P. caprinus (N = 16), clade of P. x. posticalis-P. x. rupestris (N = 155), clade of P. sp. 2 (N = 47) and clade of P. vaccarum (N = 283). Loadings of the variables, eigenvalues and proportion of the variance explained for the first 3 principal components (PC) and the first 4 discriminant functions (DF). Results are based on log10-transformed craniodental variables. See 'Material and Methods' for variable abbreviations.

analysis shows that representative specimens of this clade are, on average, the smallest of all studied populations in the eastern Andean slopes of Argentina (Table 1, Figures 8 and 9). More importantly, significant size differences, for several external and cranial traits, separate representatives of this clade from the sympatric *P. caprinus* and *P. vaccarum* clades (Supplementary Material S2), and there are even some shape differences in the skull with *P. caprinus* (Figure 9). The rounded interorbital region, the frontoparietal suture mostly 'U' shaped, the narrow rostrum and the simplified enamel molar pattern on the upper molar series are qualitative characters that also support its differentiation (Figures 2 and 3). Despite these differences, the taxonomic status of this form still needs further studies, including evaluating samples of northern Bolivia and Peru.

4.3 | The clade of *P. caprinus*

P. caprinus was described on the basis of external and skull (qualitative and quantitative) characters by Pearson (1958). Shortly after its original description, Hershkovitz (1962) considered this nominal form to be a subspecies of the polytypic *P. darwini* (along with all taxa currently allocated to the *P. xanthopygus* complex), but most of the subsequent authors retained it as different species (e.g. Cabrera, 1961; Jayat et al., 2016; Steppan, 1998; Steppan and Ramírez, 2015). The close phylogenetic relationship among *P. caprinus* and other nominal forms included in the *P. xanthopygus* species complex was first mentioned by Jayat et al. (2016) based on molecular grounds. The phylogenetic analyses conducted by Ojeda et al. (2021) consistently (in the Bayesian and the Maximum

Likelihood analyses) placed specimens of this clade as more closely related to representatives of the clade of *P. xanthopygus* s.s. (samples from Patagonia, south of the Limay river) than to specimens of the sympatric *P. x. posticalis-P. x. rupestris* and the *P. vaccarum* clades. Mean pairwise genetic distances among this and the other clades are large, between 7.7% and 10.2% (Ojeda et al., 2021), well in line with the values observed among other *Phyllotis* species (e.g. Jayat et al., 2016; Ojeda et al., 2021; Rengifo & Pacheco, 2017). The karyotype described for this taxon is nearly identical to other populations of the *P. xanthopygus* complex, having a 2n = 38, FNa = 72, with 36 size-graded biarmed autosomes, a large submetacentric X, and a small metacentric Y chromosome (Pearson & Patton, 1976). However, our morphological results are in line with the phylogenetic and genetic evidence, supporting the specific status of this nominal form. Pearson (1958: pg. 434) noted the broad rostrum and interorbital breadth of this species when compared to other *Phyllotis* species in general and with *P. xanthopygus* (=*P. darwini*) in particular. We confirm the applicability of these metric characters in separating *P. caprinus* from most other samples here studied, but also note the smaller ears, bullae, and molars of this species (Table 1). As mentioned previously, representatives of this form could be separated from sympatric populations of the clade of *P. x. posticalis-P. x. rupestris* through several qualitative (see Pearson, 1958; Steppan and Ramírez, 2015; and Figures 2 and 3) and quantitative state characters (Table 1 and Supplementary Material S2). It is morphometrically more similar to specimens of the clade of *P. vaccarum*. In addition to the morphometric characters separating them from most other samples, there are a few qualitative morphological characters (e.g. the shape of the interorbital region and the frontoparietal suture) that could be useful in separating both forms. Furthermore, all multivariate analyses including size consistently separate these two forms at different ends (of the PCII and of the DF II) of the multivariate morphometric space (Figures 8 and 9). In short, our analysis and several other sources of evidence indicate that the consideration of this nominal form as a valid species is the more strongly supported taxonomic hypothesis. This geographically restricted form inhabits a relatively small geographic area in shrubby habitats on the eastern Andean slopes of northwestern Argentina and southern Bolivia, between 2,100 and 4,500 m (Steppan & Ramírez, 2015; Figure 1) and is separate by more than 1,600 km of its sister *P. xanthopygus* s.s. in the Patagonian steppe.

4.4 | The clade of *P. vaccarum*

Phylogenies based on *cytb* have placed specimens of this clade (alternatively referred as *x. vaccarum*, or *x. rupestris* in previous studies) as sister to *P. limatus* (e.g. Albright, 2004;

Riverón, 2011; Steppan et al., 2007). Ojeda et al. (2021) corroborated this relationship after adding specimens of the nominal form *ricardulus* to the already included *rupestris* and *vaccarum*, plus specimens from additional localities of western Argentina. Genetic p-distances between *P. limatus* and the clade of *P. vaccarum* range from 2.6% to 3.7% and are the smallest distances among the eight main clades obtained by Ojeda et al. (2021). Steppan (1998) first argued for the specific status of *P. limatus* on distinctive morphology (e.g. uniquely quite narrow and deep incisors, short to moderate molar row, light coloration, belly frequently white), monophyly of the mitochondrial lineage and geographic distribution (*P. limatus* are mainly restricted to western Andean areas). Genetic sampling was however very limited in Steppan (1998). Kuch et al. (2002) and Albright (2004) suggested a recent speciation for *P. limatus*, which could be an independent lineage diverging in the last ~140,000 years. We examined specimens of *P. limatus* and corroborated its distinctiveness from specimens of the clade of *P. vaccarum* with regard to the former's quite narrow and deep incisors. Specimens referred to *P. vaccarum* from western Argentina and central Chile have differences in the amount of constitutive heterochromatin of their karyotypes when compared with individuals of *P. x. posticalis-P. x. rupestris* and *P.* sp. 2 (cf. Labaroni et al., 2014; Walker et al., 1991). Mean pairwise genetic distances between specimens of the clade of *P. vaccarum* and those of other clades within the complex of *P. xanthopygus* (excluding *limatus*) range from 7.9% to 9.7% (see Table 1 in Ojeda et al., 2021), values that are in line with other recognized species. Samples of specimens corresponding to this clade are intermediate in size between the populations here analysed, being on average larger than samples of the sympatric *P. x. posticalis-P. x. rupestris* and somewhat smaller compared with the sympatric *P.* sp. 2 (Table 1). Although specimens of this clade overlapped with samples of the *P. x. posticalis-P. x. rupestris* and the *P.* sp. 2 clades in the univariate statistic comparisons, several metric characters can be useful in segregate them (Table 1 and Supplementary Material S2). The PCA and the DFA also show this overlap (both, in size and shape of the skull), but the confusion matrix of the sDFA successfully classified more than 72% of its specimens. A more detailed quantitative and qualitative comparison of this form with representatives of *P.* sp. 2 will be developed in the following paragraphs. This clade includes specimens from several populations on eastern Andean slopes (from northern Chile and northwestern Argentina south to northeastern Neuquén Province, Argentina), three of them coming from the type localities of the nominal forms *ricardulus*, *oreigenus*, and *vaccarum*. Although we documented some morphometric differences in the univariate analysis for the nominal form *ricardulus*, size and shape multivariate analyses showed that specimens of this nominal form (and those representing *oreigenus*

and *vaccarum*) are well inside the convex hull polygons of other populations of this clade (sPCA and sfPCA analysis) or cannot be correctly classified consistently (sDFA and sfDFA) from populations coming from different geographic areas (Supplementary Material S3). Furthermore, we do not find differences in qualitative skull characters between them (Figures 4 and 5) or sharp morphometric discontinuities among populations along latitudinal or environmental gradients (Supplementary Material S3) to diagnose them as species. All evidence analysed suggests that this clade must be recognized at the species level and *vaccarum* appears as the most appropriate name for this species. Pearson (1958) used the name *rupestris* for a short tailed, small sized and pale form, distributed from southern Peru to northwestern Argentina (in Jujuy Province); in contrast, individuals we assign to *P. vaccarum* are large-bodied, long tailed and with generally more richly coloured pelage, being distributed from northern Chile and southern Jujuy, south to central Chile and west-central Argentina (cf. Pearson, 1958). Steppan (1998) argued that the location of the *rupestris* type is uncertain because the original description gives the location as 'un trou de rocher des hautes montagnes de Cobija' ('a rock hole in the high mountains of Cobija;' Gervais 1841:51) and could therefore either be near the coast in the coastal ranges east of Cobija (as argued by Heshkovitz, 1964) or high in the Andes near San Pedro de Atacama (as argued by Pearson, 1958). Both possible locations are at the extreme northwestern limit of this species, rather than near the core of the distribution, but are also within the range of *P. limatus*, a species distinguished principally by incisor shape, a trait not measured by Gervais. The type of *rupestris* is lost (Steppan, 1998), making it impossible from the available evidence to determine which species that animal was a member of. Ojeda et al. (2021) also highlighted the convenience, in terms of taxonomic stability, of referring populations of specimens representing this clade to *vaccarum* rather than *rupestris*. Consequently, we recognize *vaccarum* as the oldest available name that can be assigned to this taxon (see the taxonomic discussion in Ojeda et al., 2021 and further comments on the taxonomic account of this species in Supplementary Material S5). Here we formally recognize the specific status of this form, including a taxonomic account, an emended diagnosis, a thorough analysis of morphologic variations and a geographic distribution description for the species (Supplementary Material S5).

4.5 | The clade of *P*. sp. 2

Evidence for the recognition of this clade was first provided by phylogenetic analysis of molecular data (Albright, 2004; Riverón, 2011; Ojeda et al., 2021). In addition, specimens of *P*. sp. 2 have distinctive chromosome characteristics not detected in other clades (Labaroni et al., 2014). Teta et al. (2018) observed the morphometric similarities of populations of this clade with that of populations belonging to other clades of the *P. xanthopygus* complex. Notwithstanding, specimens of this clade were distinguishable from other species of this complex on univariate and multivariate analyses (Figures 8 and 9; Table 1 and Supplementary Material S3). These differences, complemented and integrated with other sources of evidence (e.g. genealogical relationships, genetic divergence, and karyotype characteristics), strongly indicate that this clade represents a distinct and unnamed species. Here, we describe and compare this new entity with related species of the *P. xanthopygus* complex (Supplementary Material S6). The new name was registered in the Official Register of Zoological Nomenclature (ZooBank) with number LSID urn:lsid:zoobank.org:pub:E39D9E98-CC02-4D2E-AC32-3573136FE6EE.

4.6 | Final remarks

Although we think that accumulated evidence (i.e. molecular, morphologic, cytogenetic) has contributed substantially to species delimitation of populations of the genus *Phyllotis* distributed on western Andean slops of central Argentina, undoubtedly there is a need to include additional approaches to further refine our knowledge. These must include the study of nuclear DNA sequences (the mtDNA gene tree may depart from the species tree due to lineage sorting of ancestral polymorphisms or later introgression), environmental niche preferences and the biogeographic history of these populations, among others. Similarly, there is a need for assess populations from the western side of the Andes, in particular Chilean populations, which could help to adequately delineate the species diversity of this complex species group. Small mammal diversity studies in Andean ecosystems are urgently needed in light of major threats (e.g. habitat degradation associated to open mining operations, biological invasions, cattle overgrazing, exotic species and climate change; Ceballos & Ehrlich, 2006; Nuñez et al., 2009; Reborati, 2005; Zapata-Ríos & Branch, 2016). Even when the systematics of the leaf-eared mice is one of the most studied in South America, the description of the new species, *P. pehuenche* new sp., highlights a common theme in Neotropic mammalogy. That is, the need to fulfil the Linnean deficit through exploration and description of the tremendous diversity of small mammals within a phylogenetic and integrative taxonomic framework, particularly for those complexes of almost morphologically cryptic species.

ORCID

J. Pablo Jayat 🆔 https://orcid.org/0000-0002-6838-2987

REFERENCES

Albright, J. C. (2004). *Phylogeography of the sigmodontine rodent,* Phyllotis xanthopygus*, and a test of the sensitivity of nested clade analysis to elevation–based alternative distances*. M.S. Thesis. The Florida State University. 46 pp.

Barbière, F., Ronez, C., Ortiz, P. E., Martin, R. A., & Pardiñas, U. F. J. (2019). A new nomenclatural system for the study of sigmodontine rodent molars: First step towards an integrative phylogeny of fossil and living cricetids. *Biological Journal of the Linnean Society*, *127*, 224–244. https://doi.org/10.1093/biolinnean/blz021

Cabrera, A. (1926). Dos roedores nuevos de las montañas de Catamarca. *Revista Chilena De Historia Natural*, *30*, 319–321.

Cabrera, A. (1961). Catálogo de los mamíferos de América del Sur. *Revista del Museo Argentino de Ciencias Naturales "Bernardino Rivadavia". Ciencias Zoológicas*, *4*, 309–732.

Ceballos, G., & Ehrlich, P. R. (2006). Global mammal distributions, biodiversity hotspots, and conservation. *Proceedings of the National Academy of Sciences of the United States of America*, *103*(51), 19374–19379. https://doi.org/10.1073/pnas.0609334103

Crespo, J. A. (1964). Descripción de una nueva subespecie de roedor filotino. *Neotrópica*, *10*, 99–101.

Darriba, D., Taboada, G. L., Doallo, R., & Posada, D. (2012). jModelTest 2: More models, new heuristics and parallel computing. *Nature Methods*, *9*, 772. https://doi.org/10.1038/nmeth.2109

Ferro, L. I., Martínez, J. J., & Barquez, R. M. (2010). A new species of Phyllotis (Rodentia, Cricetidae, Sigmodontinae) from Tucumán Province, Argentina. *Mammalian Biology*, *75*, 523–537. https://doi.org/10.1016/j.mambio.2009.09.005

Frontier, S. (1976). Etude de la decroissance des valeurs propres dans une analyse en composantes principales: Comparaison avec le modele du baton brise. *Journal of Experimental Marine Biology and Ecology*, *25*, 67–75. https://doi.org/10.1016/0022-0981(76)90076-9

Hammer, O., Harper, D. A. T., & Ryan, P. D. (2001). Past: Paleontological statistics software package for education and data analysis. *Palaeontologia Electronica*, *4*, 1–9.

Hershkovitz, P. (1962). Evolution of Neotropical cricetine rodents (Muridae) with special reference to the phyllotine group. *Fieldiana Zoology*, *46*, 1–524. https://doi.org/10.5962/bhl.title.2781

Hubbs, C. L., & Hubbs, C. (1953). An improved graphical analysis and comparison of series of samples. *Systematic Zoology*, *2*(2), 49–56. https://doi.org/10.2307/2411659

Jackson, D. A. (1993). Stopping rules in principal components analysis: A comparison of heuristical and statistical approaches. *Ecology*, *74*, 2204–2214. https://doi.org/10.2307/1939574

Jayat, J. P., D'Elia, G., Pardiñas, U. F. J., & Namen, J. G. (2007). A new species of *Phyllotis* (Rodentia, Cricetidae, Sigmodontine) from the upper montane forest of the Yungas of northwestern Argentina. In: D. A. Kelt, E. P. Lessa, J. Salazar-Bravo, & J. L. Patton (eds.). *The quintessential naturalist: honoring the life and legacy of Oliver P. Pearson*, pp. 775–798. University of California, Publications in Zoology, 134. https://doi.org/10.1525/california/9780520098596.003.0022

Jayat, J. P., Ortiz, P. E., González, F. R., & D'Elía, G. (2016). Taxonomy of the *Phyllotis osilae* species group in Argentina; the status of the "Rata de los nogales" (*Phyllotis nogalaris* Thomas, 1921; Rodentia: Cricetidae). *Zootaxa*, *4083*, 397–417. https://doi.org/10.11646/zootaxa.4083.3.5

Kuch, M., Rohland, N., Betancourt, J. L., Latorre, C., Steppan, S., & Poinar, H. N. (2002). Molecular analysis of a 11 700–year–old rodent midden from the Atacama Desert, Chile. *Molecular Ecology*, *11*, 913–924. https://doi.org/10.1046/j.1365-294X.2002.01492.x

Kumar, S., Stecher, G., Li, M., Knyaz, C., & Tamura, K. (2018). MEGA X: Molecular evolutionary genetics analysis across computing platforms. *Molecular Biology and Evolution*, *35*(6), 1547–1549. https://doi.org/10.1093/molbev/msy096

Labaroni, C. A., Malleret, M. M., Novillo, A., Ojeda, A., Rodriguez, D., Cuello, P., Ojeda, R., Marti, D., & Lanzone, C. (2014). Karyotypic variation in the Andean rodent *Phyllotis xanthopygus* (Waterhouse, 1837) (Rodentia, Cricetidae, Sigmodontinae). *Comparative Cytogenetics*, *8*, 369–381. https://doi.org/10.3897/CompCytogen.v8i4.8115

Libardi, G. S., & Percequillo, A. R. (2016). Variation of craniodental traits in russet rats *Euryoryzomys russatus* (Wagner, 1848) (Rodentia: Cricetidae: Sigmodontinae) from Eastern Atlantic Forest. *Zoologischer Anzeiger – A Journal of Comparative Zoology*, *262*, 57–74. https://doi.org/10.1016/j.jcz.2016.03.005

Maddison, W. P., & Maddison, D. R. (2017). *Mesquite: A modular system for evolutionary analysis*. Available Online at: http://mesquiteproject.org

Meachen-Samuels, J., & Van Valkenburgh, B. (2009). Craniodental indicators of prey size preference in the Felidae. *Biological Journal of the Linnean Society*, *96*, 784–799. https://doi.org/10.1111/j.1095-8312.2008.01169.x

Myers, P. (1989). A preliminary revision of the *varius* group of *Akodon* (*A. dayi, dolores, molinae, neocenus, simulator, toba* and *varius*). In K. H. Redford, & J. F. Eisenberg (ed.), *Advances in neotropical mammalogy* (pp. 5–54). Sandhill Crane Press, Inc.

Myers, P., Patton, J. L., & Smith, M. F. (1990). A review of the *boliviensis* group of *Akodon* (Muridae: Sigmodontinae) with emphasis on Peru and Bolivia. *Miscellaneous Publications of the Museum of Zoology, University of Michigan*, *177*, 1–89.

Nuñez, M. N., Solman, S. A., & Cabre, M. F. (2009). Regional climate change experiments over southern South America. II: Climate change scenarios in the late twenty-first century. *Climate Dynamics*, *32*, 1081–1095. https://doi.org/10.1007/s00382-008-0449-8

Ojeda, A. A., Teta, P., Jayat, J. P., Lanzone, C., Cornejo, P., Novillo, A., & Ojeda, R. A. (2021). Phylogenetic relationships among cryptic species of the *Phyllotis xanthopygus* complex (Rodentia, Cricetidae). *Zoologica Scripta*, *50*, 269–281. https://doi.org/10.1111/zsc.12472

Pacheco, V., Rengifo, E. M., & Vivas, D. (2014). Una nueva especie de ratón orejón del género *Phyllotis* Waterhouse, 1837 (Rodentia:

Cricetidae) del norte del Perú. *Therya*, *5*, 81–508. https://doi.org/10.12933/therya-14-185

Pearson, O. P. (1958). A taxonomic revision of the rodent genus *Phyllotis*. *University of California, Publications in Zoology*, *56*, 391–496.

Pearson, O. P. (1972). New Information on ranges and relationships within the rodent genus *Phyllotis* in Peru and Ecuador. *Journal of Mammalogy*, *53*, 677–686. https://doi.org/10.2307/1379206

Pearson, O. P., & Patton, J. L. (1976). Relationships among South American phyllotine rodents based on chromosome analysis. *Journal of Mammalogy*, *57*, 339–350. https://doi.org/10.2307/1379693

Reborati, C. (2005). Situación ambiental en las ecorregiones Puna y Altos Andes. In: A. Brown, U. Martinez Ortiz, M. Acerbi, & J. Corcuera (eds.). *La Situación Ambiental Argentina 2005* (pp. 32–47), Fundación Vida Silvestre Argentina.

Reig, O. A. (1978). Roedores cricétidos del Plioceno superior de la provincia de Buenos Aires (Argentina). *Publicaciones Del Museo Municipal De Ciencias Naturales De Mar Del Plata Lorenzo Scaglia*, *2*, 164–190.

Rengifo, E. M., & Pacheco, V. (2015). Taxonomic revision of the Andean leaf–eared mouse, *Phyllotis andium* Thomas 1912 (Rodentia: Cricetidae), with the description of a new species. *Zootaxa*, *4018*, 349–380. https://doi.org/10.11646/zootaxa.4018.3.2

Rengifo, E. M., & Pacheco, V. (2017). Phylogenetic position of the Ancash leaf-eared mouse *Phyllotis definitus* Osgood 1915 (Rodentia: Cricetidae). *Mammalia*, *82*, 153–166. https://doi.org/10.1515/mammalia-2016-0138

Riverón, S. (2011). *Estructura poblacional e historia demográfica del "pericote patagónico" Phyllotis xanthopygus (Rodentia: Sigmodontinae) en Patagonia Argentina*. Ph. D. Dissertation (pp. 100). Uruguay: Universidad de la República.

Sievers, F., Wilm, A., Dineen, D., Gibson, T. J., Karplus, K., Li, W., Lopez, R., McWilliam, H., Remmert, M., Söding, J., Thompson, J. D., & Higgins, D. G. (2011). Fast, scalable generation of high-quality protein multiple sequence alignments using Clustal Omega. *Molecular Systematics and Biology*, *7*, 539. https://doi.org/10.1038/msb.2011.75

Stamatakis, A. (2006). RAxML-VI-HPC: Maximum likelihood-based phylogenetic analyses with thousands of taxa and mixed models. *Bioinformatics*, *22*, 2688–2690. https://doi.org/10.1093/bioinformatics/btl446

Steppan, S. J. (1993). Phylogenetic relationships among the Phyllotini (Rodentia: Sigmodontinae) using morphological characters. *Journal of Mammalian Evolution*, *1*, 187–213. https://doi.org/10.1007/BF01024707

Steppan, S. J. (1995). Revision of the tribe Phyllotini (Rodentia: Sigmodontinae), with a phylogenetic hypothesis for the Sigmodontinae. *Fieldiana Zoology, New Series*, *80*, 1–112. https://doi.org/10.5962/bhl.title.3336

Steppan, S. J. (1998). Phylogenetic relationships and species limits within *Phyllotis* (Rodentia: Sigmodontinae): Concordance between mtDNA sequence and morphology. *Journal of Mammalogy*, *7*, 573–593. https://doi.org/10.2307/1382988

Steppan, S. J., & Ramírez, O. (2015). Genus Phyllotis Waterhouse, 1837. In: J. L. Patton, U. F. J. Pardiñas, & G. D'Elía (eds.). *Mammals of South America, Volume 2, Rodents* (pp. 535–555), The University of Chicago Press Chicago and London. https://doi.org/10.7208/chicago/9780226169606.001.0001

Steppan, S. J., Ramirez, O., Banbury, J., Huchon, D., Pacheco, V., Walker, L. I., & Spotorno, A. E. (2007). A molecular reappraisal of the systematics of the leaf–eared mice *Phyllotis* and their relatives. In D. A. Kelt, E. P. Lessa, J. Salazar-Bravo, & J. L. Patton (Eds.), *The Quintessential Naturalist: Honoring the Life and Legacy of Oliver P. Pearson* (pp. 799–826). University of California, Publications of Zoology. https://doi.org/10.1525/california/9780520098596.001.0001

Storz, J. F., Quiroga-Carmona, M., Opazo, J. C., Bowen, T., Farson, M., Steppan, S. J., & D'Elia, G. (2020). Discovery of the world's highest-dwelling mammal. *Proceedings of the National Academy of Sciences of the United States of America*, *117*, 18169–18171. https://doi.org/10.1073/pnas.2005265117

Teta, P., Jayat, J. P., Lanzone, C., Novillo, A., Ojeda, A., & Ojeda, R. A. (2018). Geographic variation in quantitative skull traits and systematics of southern populations of the leaf-eared mice of the *Phyllotis xanthopygus* complex (Cricetidae, Phyllotini) in southern South America. *Zootaxa*, *4446*, 68–80. https://doi.org/10.11646/zootaxa.4446.1.5

Thomas, O. (1912). New bats and rodents from S. America. *The Annals and Magazine of Natural History*, *8*(10), 403–411.

Thomas, O. (1919). On small mammals from "Otro Cerro", north- eastern Rioja, collected by Sr. E. Budin. *The Annals and Magazine of Natural History*, *9*(3), 489–500.

Walker, L. I., Spotorno, A. E., & Arrau, J. (1984). Cytogenetic and reproductive studies of two nominal subspecies of Phyllotis darwini and their experimental hybrids. *Journal of Mammalogy*, *65*, 220–230. https://doi.org/10.2307/1381161

Walker, L. I., Spotorno, A. E., & Sans, J. (1991). Genome size variation and its phenotypic consequences in *Phyllotis* rodents. *Hereditas*, *115*, 99–107. https://doi.org/10.1111/j.1601-5223.1991.tb03542.x

Zapata-Ríos, G., & Branch, L. C. (2016). Altered activity patterns and reduced abundance of native mammals in sites with feral dogs in the high Andes. *Biological Conservation*, *193*, 9–16. https://doi.org/10.1016/j.biocon.2015.10.016

SUPPORTING INFORMATION

Additional supporting information may be found online in the Supporting Information section.